Simple Route for Synthesis of PbS Dendritic Nanostructured Materials

Qing Huang and Lian Gao*
State Key Laboratory of High Performance Ceramics and Superfine Microstructure, Shanghai Institute of Ceramics, Chinese Academy of Sciences, Shanghai 200050, P. R. China

(Received July 26, 2004; CL-040871)

Novel PbS dendritic nanostructured materials are synthesized using 2-aminoethanethiol (AET) via simple hydrothermal approach. The morphology evolution of PbS from zero-dimensional nanodots, one-dimensional rod-shaped structure to three-dimensional dendritic nanostructure is well illustrated and explained in terms of the adsorption of AET molecule on the crystal surface.

PbS is a very important semiconducting material and has potential application as photoelectric switching devices because of its narrow band gap energy (0.41 eV) and large exciton Bohr radius (18 nm).[1] Hence, great attention has been paid on this special chalcogenide, especially on its morphology-controlled synthesis. Cheon et al. studied the shape evolution ranging from anisotropic to isotropic forms, and found unusual transient multipod forms.[2] Qian et al. systematically investigated the effect of additives on the morphology of resulting PbS crystals.[3–5] Close-bundled PbS nanowires with regular geometric shapes were synthesized in the presence of poly[*N*-(2-aminoethyl)acrylamide].[6] Recently, novel dendritic PbS crystal was also reported.[7,8] However, the morphology evolution of PbS crystal with this novel structure is not fully revealed and further studies are indispensable to elucidate the crystal growth habit. Herein, with the 2-aminoethanethiol as the sulphur resource, we observed that the morphologies of the PbS crystals could be effectively controlled by modulating the reaction temperature. PbS crystals with dot, rod, multipod-shaped morphologies and fishbone-shaped dentritic microstructures can be synthesized without surfactant.

The chemicals used were analytical grade. Typically, 3 mmol of lead acetate ($Pb(CH_3COO)_2 \cdot 3H_2O$, Shanghai Chemical Reagent Co., Ltd), 20 mmol of NaOH and 12 mmol of 2-aminoethanethiol (AET; $HSCH_2CH_2NH_2$, ACROS ORGANICS) were added into 30-mL distilled water where the mol ratio of Pb and AET remained 1:4. AET will be reactive and release S^{2-} under alkaline condition. After stirring for 5 min, this solution was transferred into a 35-mL Teflon-lined stainless-steel autoclave and was hydrothermally treated at 80–180 °C for 6 h. The final products were filtered out, washed with distilled water and ethanol in subsequence, and later dried in vacuum oven at 60 °C for 12 h.

The products were characterized by using X-ray powder diffraction (XRD, D/max 2550V) with Cu Kα radiation (λ = 0.15406 nm). High-resolution transmission electron microscopy (HRTEM) images were taken on TEM (JEM-2010, 200 kV) with EDX attachment. Scanning electron micrograph was obtained using field emission scanning electron microscopy (FE-SEM, JSM-6700F, 15 kV). X-ray photoelectron spectroscopic measurement was performed on a Microlab MKII spectrometer with Mg Kα radiation (electron power: 300 W).

Figure 1 shows the X-ray diffraction spectra of products obtained at different temperatures. At low temperature (Figures 1a and 1b) lead sulfide (JCPDS 05-0592) coexisting with the lead carbonate hydroxide hydrate phases (JCPDS 9-0356) was formed. When the temperature was increased to 110 °C, pure PbS crystals were obtained (Figure 1c). Thus, we proposed following reactions accounting for the phase transformation at different temperatures.

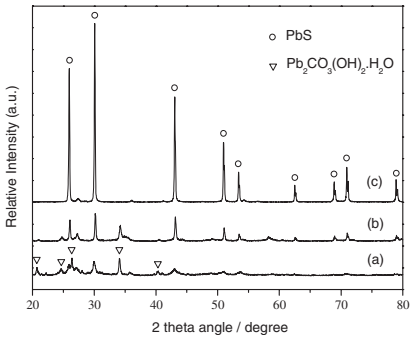

Figure 1. XRD patterns of products reacted at (a) 60 °C, (b) 80 °C, and (c) 110 °C.

$$4Pb^{2+} + 4CH_3COO^- + 4OH^- + 4H_2O \xrightarrow{\text{low temperature}} 2PbCO_3 \cdot Pb(OH)_2 \cdot H_2O\downarrow + 4CH_4\uparrow + 2CO_3^{2-} \quad (1)$$

$$Pb^{2+} + HSCH_2CH_2NH_2 + 2OH^- \xrightarrow{\text{high temperature}} PbS\downarrow + HOCH_2CH_2NH_2 + H_2O \quad (2)$$

The morphology evolution is depicted in Figure 2. At low temperature, well-dispersed PbS nanodots were formed and self-assembling hexagonal shape was preferred (Figure 2a). The diffraction rings indexed as (111), (200), (220), and (311) crystal planes in selected area electron diffraction (SAED, inset in the Figure 2a) pattern, confirmed that the particles were lead sulfide. The average grain size of lead sulfide nanocrystals is about 12 nm (Figures 2a and 2b), which consists with the value 14 nm determined from the broadening of the (110) peak by the Scherrer formula: $L = 0.89\lambda/\beta\cos\theta$. The (200) crystal lattice is clearly shown in the high-resolution transmission electron microscopy (HRTEM) image (Figure 2b). When the temperature was increased to 110 °C, the major product was rod-shaped crystals with an aspect ratio of 8 ($\pm$1.4, 50 rods were calculated, 85%, Figure 2c) accompanied with tetrapod-shaped (10%, Figure 2d) and hexapod-shaped (5%, Figure 2e) crystals. All the products are in the first-order crystal structure. The growth direction of rods (or pods) is along the orientations of $\langle 100 \rangle$ on the basis of the SAED characterization. Elevating the temperature to 150 °C, second-order dendritic structure emerged. Figure 2f shows that some short subrods perpendicularly grow on the main crystals. The width and length of subrod are about 100 and

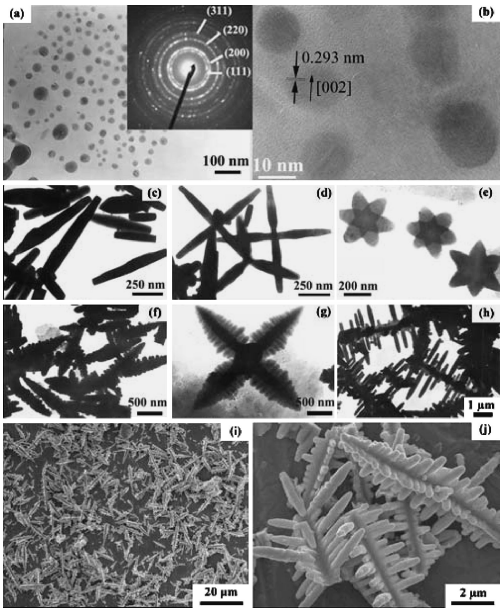

Figure 2. TEM image of products synthesized at 80 °C (a) and its corresponding HRTEM image (b). TEM images of products synthesized at (c)–(e) 110 °C, (f) and (g) 150 °C, and (h) 180 °C. (i) Low magnitude and (j) high magnitude SEM images of dendritic PbS crystals synthesized at 180 °C.

250 nm, respectively. Simultaneously, dendritic structure also exists in the tetrapod-shaped crystal (Figure 2g). By further increasing the reaction temperature to 180 °C, the dendritic structure becomes more evident (Figure 2h). The width and length of subrods increase to about 250 nm and 1.5 μm, respectively. FE-SEM image shows the fishbone-like microstructure of dendritic PbS crystals (Figure 2i). Figure 2j clearly presents the fine structure that four arrays of subrods perpendicularly protrude out from main trunk of crystals. If the direction of main trunk is ⟨100⟩ orientation, these four branches should be indexed as ±⟨010⟩ and ±⟨001⟩ orientation.

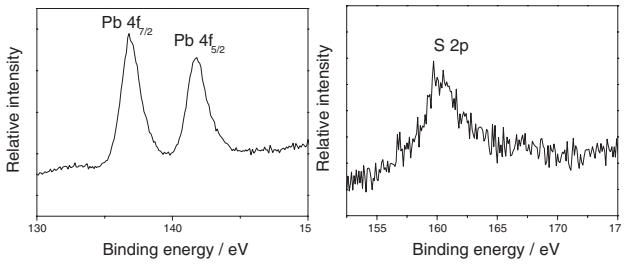

Figure 3. XPS spectra of PbS sample synthesized at 110 °C.

Although a few works have been reported on this novel micropattern of PbS, the exact formation mechanism has not been understood.[7,8] From our observation of morphology evolution at different synthesis temperatures, we propose that the adsorption of AET molecules on crystal planes of PbS may play an important role to determine the final microstructure. At the initial nucleation stage, $PbCO_3 \cdot Pb(OH)_2 \cdot H_2O$ is firstly precipitated and consequently reacted with S^{2-} anions released from AET under alkaline condition to form PbS nuclei. AET molecule should be considered as a bifunctional ligand in which S atoms can strongly interact with PbS surface, whereas NH_2 groups stretch into solution although there also exist some possibilities that NH_2 groups can interact with Pb ions. X-ray photoelectron spectroscopy (XPS) was applied to characterize the surface state of PbS crystals (Figure 3). The measured sample was synthesized at 110 °C. The core-level binding energies of Pb (136.80 eV for $4f_{7/2}$ and 141.80 eV for $4f_{5/2}$) and S (159.7 eV for 2p) are well consistent with the reference values of PbS.[9] Atomic ratio of Pb and S calculated from peak areas is about 1:2.5, which corroborates the adsorption of AET (or resultant aminoethanol) on the surface of PbS particles. In the reference sample that precipitated from $PbCl_2$ and Na_2S, the atomic ratio of Pb/S is nearly 1:1. IR spectrum (not shown here) of the product further confirms the existence of N–H groups (1608 cm^{-1}) after reaction. Thus, it is tentative to phenomenologically explain the formation of isotropic nanodots at low temperature because the AET molecule tightly caps on the surface of crystal nuclei. The nanodots repulse each other for the space-blocking effect of capping molecules. When the temperature increases, thermal disturbance becomes violent. On the lattice surface with low index (such as {100}), the interaction strength between AET and PbS should be weak for the low charge density. Thus, AET molecule will be desorbed and expose these low-index surfaces. Correspondingly, the growth on these faces will be enhanced. Although {100} faces are low-energy faces in the rock-salt type crystal, they are kinetically favored in our case because other faces are capped by AET molecule. This argument is consistent with the explanation for formation of PbS nanocrystals with varied morphology proposed by Lee et al., in which dodecanethiol was used to adsorb on the surface of PbS nanocrystal and tune the growth rate of varied faces.[2] It is also revealed that activation barrier of {100} faces should be lower than that of {111} faces at high temperature, which results in star-like nanocrystals. When these rod-like or star-like crystals grow large, sub-branch crystals will nucleate and grow on these trunks and form dendritic pattern.

In summary, PbS with various morphologies including nanodots, nanorods, and dendritic microstructure, can be successfully synthesized at different temperatures using AET molecule both as sulfur source and capping ligand via hydrothermal treatment. The morphology evolution of PbS is phenomenologically proposed in terms of adsorption of AET molecule on the crystal surface. This novel approach to synthesize shape-tunable PbS crystals enriches the inorganic synthesis and crystal growth knowledge.

We acknowledge Meiling Ruan for her guidance and help with the TEM work.

References

1 L. Brus, *J. Phys. Chem. B*, **90**, 2555 (1986).
2 S. M. Lee, Y. W. Jun, S. N. Cho, and J. W. Cheon, *J. Am. Chem. Soc.*, **124**, 11244 (2002).
3 M. Chen, Y. Xie, Z. Yao, Y. T. Qian, and G. Zhou, *Mater. Res. Bull.*, **37**, 247 (2002).
4 D. Wang, D. Yu, M. S. Mo, X. M. Liu, and Y. T. Qian, *Solid State Commun.*, **125**, 475 (2003).
5 D. Yu, D. B. Wang, S. S. Zhang, X. M. Liu, and Y. T. Qian, *J. Cryst. Growth*, **249**, 195 (2003).
6 D. Yu, D. B. Wang, Z. Y. Meng, J. Liu, and Y. T. Qian, *J. Mater. Chem.*, **12**, 403 (2002).
7 D. B. Wang, D. B. Yu, D. B. Yu, M. W. Shao, X. M. Liu, W. C. Yu, and Y. T. Qian, *J. Cryst. Growth*, **257**, 384 (2003).
8 D. Kuang, A. Xu, Y. Fang, H. Liu, C. Frommen, and D. Fenske, *Adv. Mater.*, **15**, 1747 (2003).
9 "Handbook of X-ray Photoelectron Spectroscopy," ed. by G. E. Muilenberg, C. D. Wager, W. M. Riggs, L. E. Davis, and J. F. Moulder, Perking-Elmer, New York (1979).

Published on the web (Advance View) September 18, 2004; DOI 10.1246/cl.2004.1338